CHAPTER 193

A Three Dimensional Model of the Gulf of Alaska

Shiao-Kung Liu and Jan J. Leendertse

Abstract

This paper presents the development of a three dimensional model of the Gulf of Alaska. The model extends between the Vancouver Island and the Aleutian Islands covering approximatedly 1.5 million square kilometers over the northern Pacific Ocean. Formulated on an ellipsoidal horizontal grid and variable vertical grid, the model is schematized over a 81 x 53 x 10 grid structure. The solution scheme is implicit over the vertical and is programmed using one-dimensional dynamic array for the efficient use of machine storage. The turbulence closure scheme for the non-homogeneous vertical shear is formulated so that the potential and kinetic energetics are monitored and transferred in a closed form.

The hydrodynamic model is coupled to a two-dimensional stochastic weather model and an oil-spill trajectory/weathering model. The former also simulates stochastically the cyclogenetic/cyclolytic processes within the modeled area.

The paper also compares the computed results with the available field data. Good agreements are found in tidal amplitude and phases as well as currents.

The Three-Dimensional Modeling System

The model of the Gulf of Alaska uses a modeling system which consists of a three-dimensional hydrodynamic model, a two-dimensional stochastic/deterministic weather model, and an oil spill trajectory/weathering model (Fig 1).

The hydrodynamic model is formulated according to the equations of motion for water and ice, continuity, state, the balance of heat, salt, pollutant and turbulent energy densities on a three-dimensional variable grid. In the vertical, the momentum and constituent transport over the variable layers are solved implicitly. The horizontal grid network coincides with the global ellipsoidal system and has a one-to-one mapping to a Mercator projection for graphical outputs. The derivation of the model equation and the comparison between other layered models are available in the open literature, eg. Liu and Leendertse, 1978, in which aspects such as open boundary conditions, numerical stability, solution discontinuity, and conservation properties are also discussed.

The RAND Corporation, Santa Monica, Calif. 90406, U. S. A.

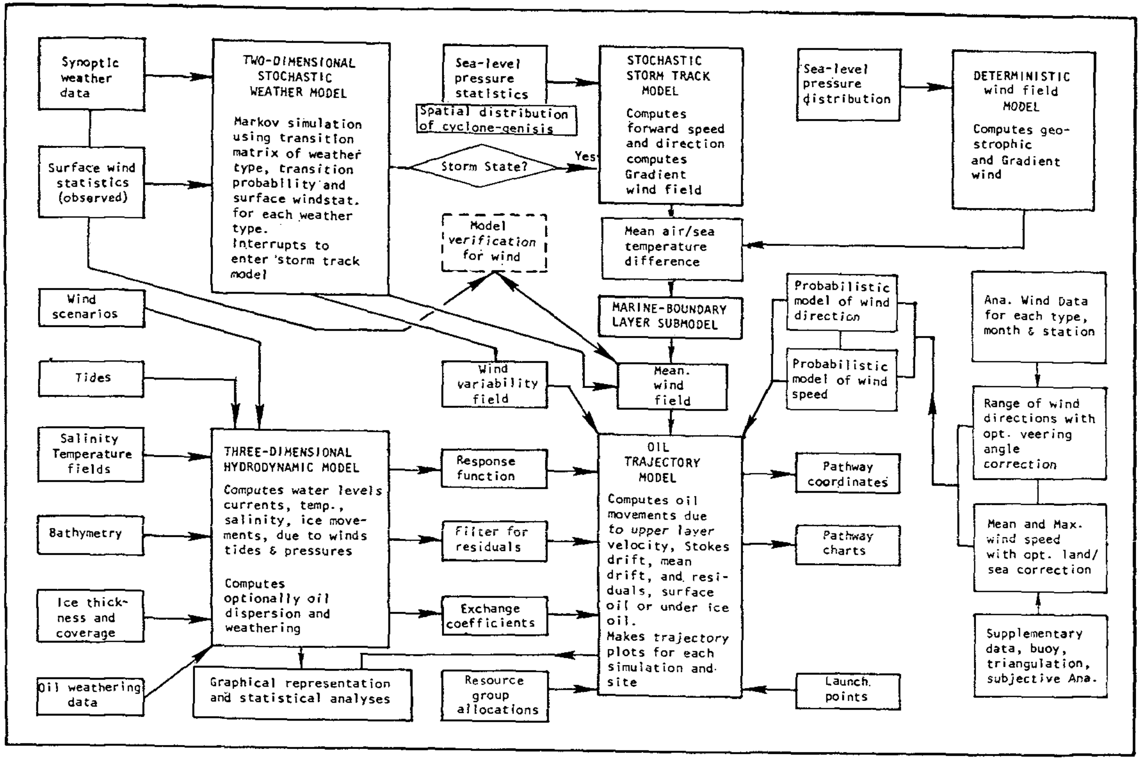

Fig. 1-- Information flow chart showing that both the three-dimensional hydrodynamic and the weather model provide important parameters needed by the oil-spill trajectory model. These parameters are difficult and expensive to measure over the entire coastal waters. Observed wind roses, if available, can still be used to drive the trajectory model in its simplist mode.

In the vertical turbulence-closure scheme, the energy production term from the surface layer is computed from the parameterization of the wind-wave generation mechanism. This approach thus circumvents certain difficulties associated with the traditional two-equation model in which a symmetry condition is assumed (as a moving wall, same as the bottom).

The model is capable of having arbitrary layer number and layer thickness, therefore minimizes numerical (pseudo) mixing in deep water. In deep water, the stratification is usually more pronounced than in the shallower, well-mixed areas.

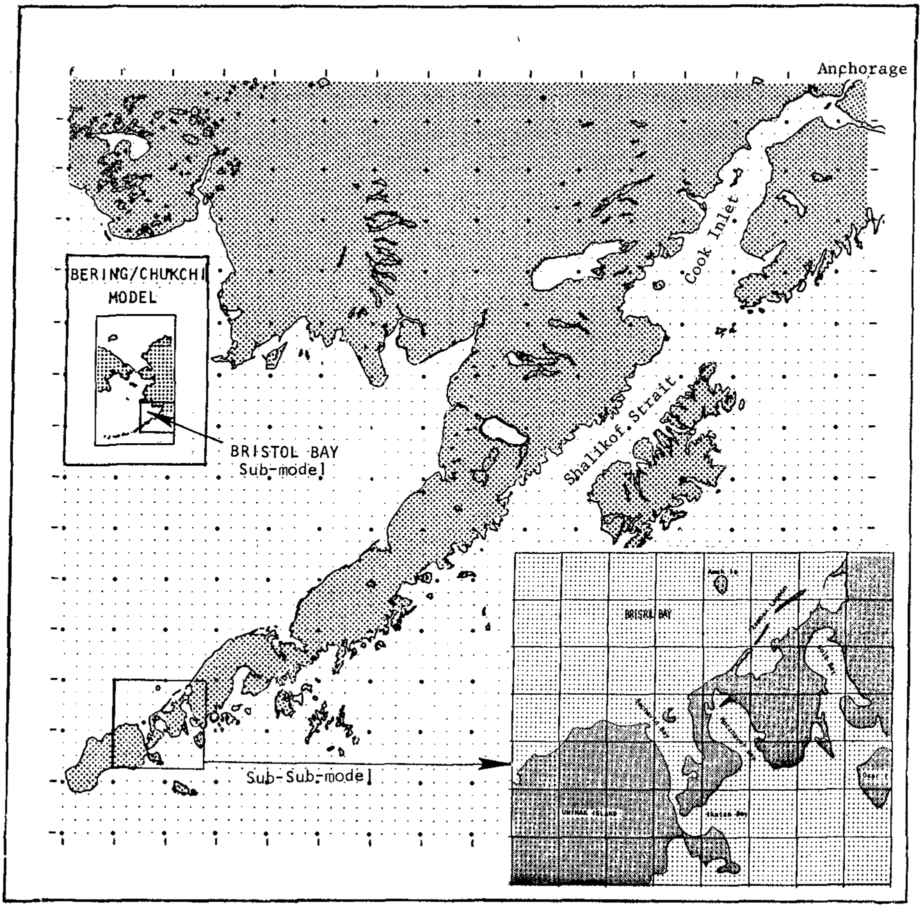

Fig. 2-- A sub-model of Bering Sea covering the area of Bristol Bay and a portion of the Gulf of Alaska. Insert map at the lower left corner is another sub-model of this one, covering the area of Izembak Lagoon.

The model of the Gulf of Alaska

The model of the Gulf of Alaska is the largest model covering the Alaskan coastal waters developed by the authors. Alaskan coast line stretches longer than the other states of the continental U. S. combined. Because of the complex coastal features, a series of nested submodels are needed to resolve the circulation dynamics of the near shore lagoons and the ecologically sensitive passages (Fig. 2). The nested models derive their boundary condition from the larger model because conducting field work in Alaska is both difficult and expensive. The embayment in the NE corner of Fig. 2 is the Cook Inlet, where the largest astronomical tides in the Pacific are found; sometimes reaching 13 meters. Also present are the strong currents and residual circulation induced by the nonlinear interaction between the advective mechanism and bethymetry of the coast.

The three dimensional perspective diagram in the upper part of Fig. 3 illustrates the along-shore view of the higher modes in the water level variation with the highest point at the head of Cook Inlet while the lower diagram shows the cross-shore variations.

Figure 4 shows the computed co-tidal chart for the semidiurnal component and the comparison between the computed amplitudes and phases at four locations where observed data are avaliable (Schumacher and Muench, 1980). Fig. 5 through 8 present the computed horizontal/vertical velocity components and the turbulent energy intensities at levels 1,3,5,7,8,9 at a location near the openning of Cook Inlet (Portlock Bank). At that location, the computed hodograph in Fig 9 nearly matches the observed current ellipse.

The computed tidal ellipses for the entire Gulf of Alaska, from Vancouver Island to the Aleutian Islands are presented in Fig. 10. In order to show the strong tidal currents within the Cook Inlet and over shelf areas, the plotting scale is set at 200 cm/sec per grid spacing. The maxmum tidal excursions are found in the middle of Cook Inlet where the tidal currents can reach 140 cm/sec in either direction. Currents over the shelf break can also reach 70 cm/sec. The computed tidal residual current distribution within the Gulf of Alaska is presented in Fig 11. In the figure, the maximum residual current in Cook Inlet is approximately 7.5 cm/sec, which is 5.5 percent of the local maximum tidal current. Over the shelf and in the Shalikof Strait, the direction of the residual current is primarily to the southwest.

Model Behavior and Discussion

In stratified geophysical flow, the density-induced vertical exchange often has a time scale much shorter than its horizontal baroclinic counterpart. It also plays an important role in the coastal ecological balance via the euphotic/energetic processes.

It therefore creates stringent demands on the accuracy of modeling. On one hand, advances made in other discipline, such as the aerodynamic modeling, can often be applied to the geophysical flows, but, on the other hand, the differences in the free-surface and other boundary treatments makes the closure technique not necessarily identical for stratified flows. Specially

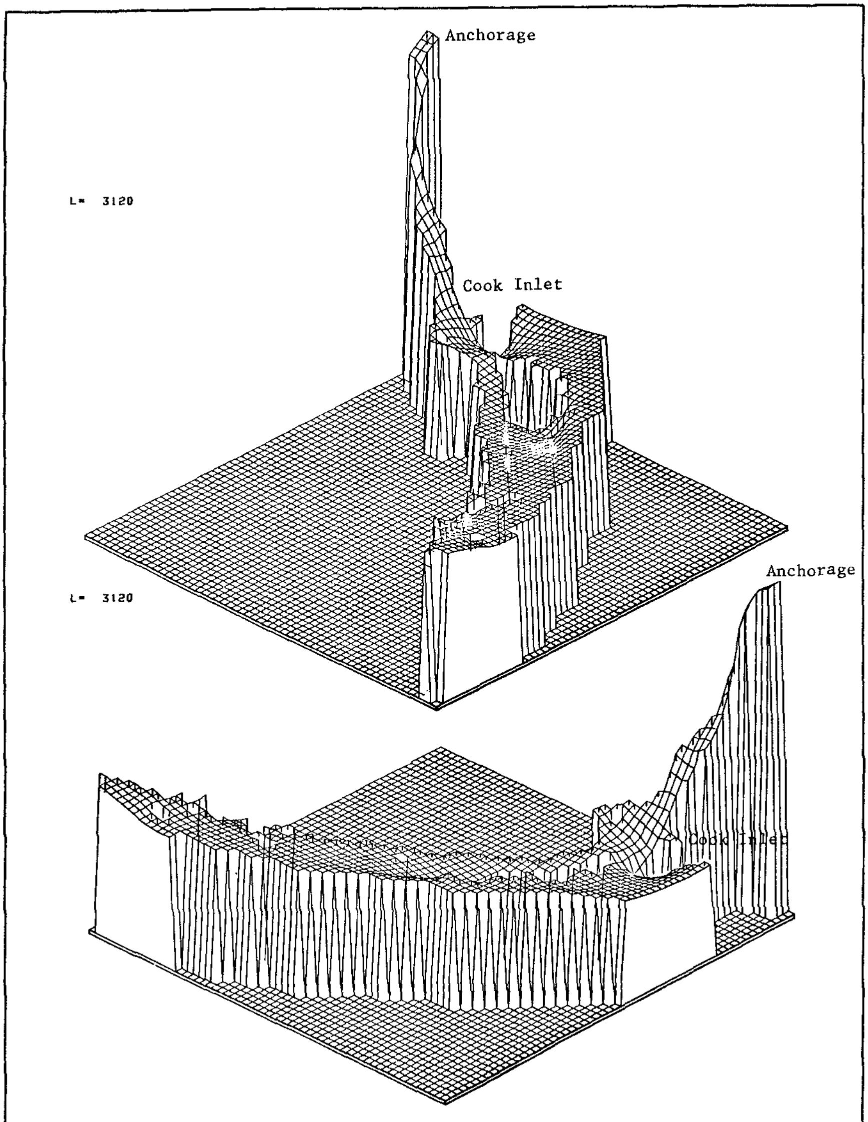

Fig. 3--Three-dimensional perspective diagrams illustrate the along-shore view of higher modes in the water level variation with the highest point at the head of Cook Inlet near Anchorage (upper diagram). The lower diagram shows the cross-shore variation.

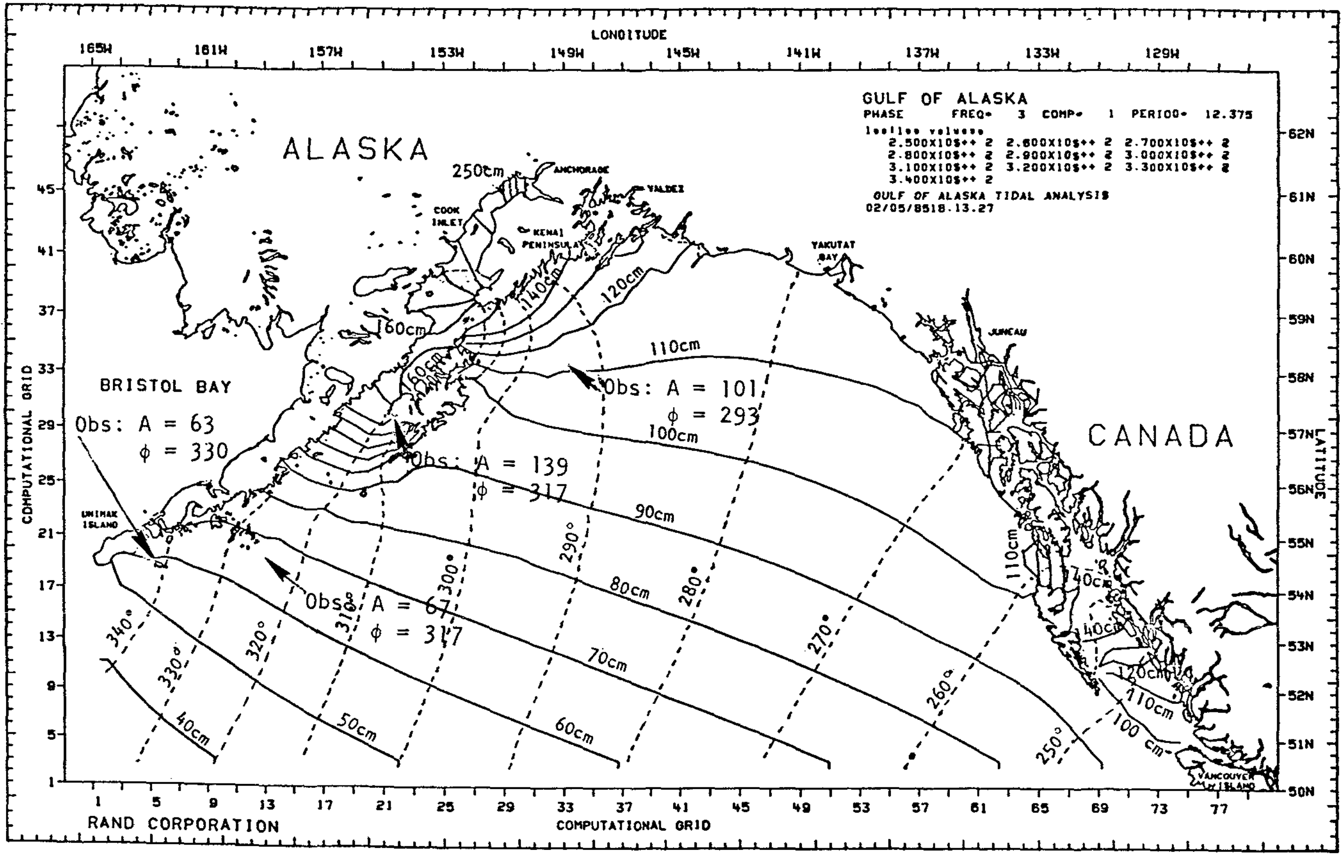

Fig. 4-- Computed co-tidal chart for the semi-diurnal component (primarily M2). Each ten degrees in phase represents approximately 20 minutes lag relative to the Greenwich mean phase. The maximum tidal amplitues are found in the Cook Inlet reaching 250 cm.

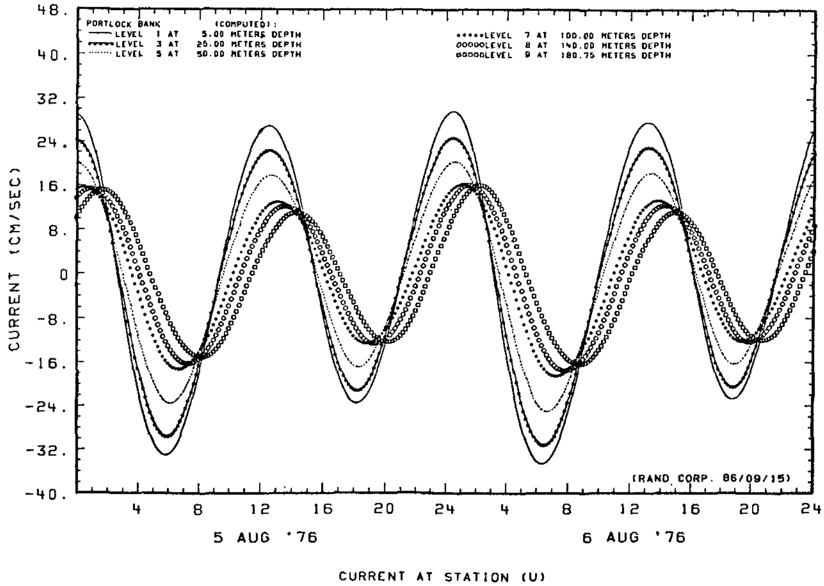

Fig. 5--The computed east-west velocity components at six representative layers near the mouth of Cook Inlet (Portlock Bank).

(GULF.TIDE.T8=XXXX.T9=8077.T10=9312.T14=XXXX) (86/05/10 16.06.58 86/09/09 18:13:30)

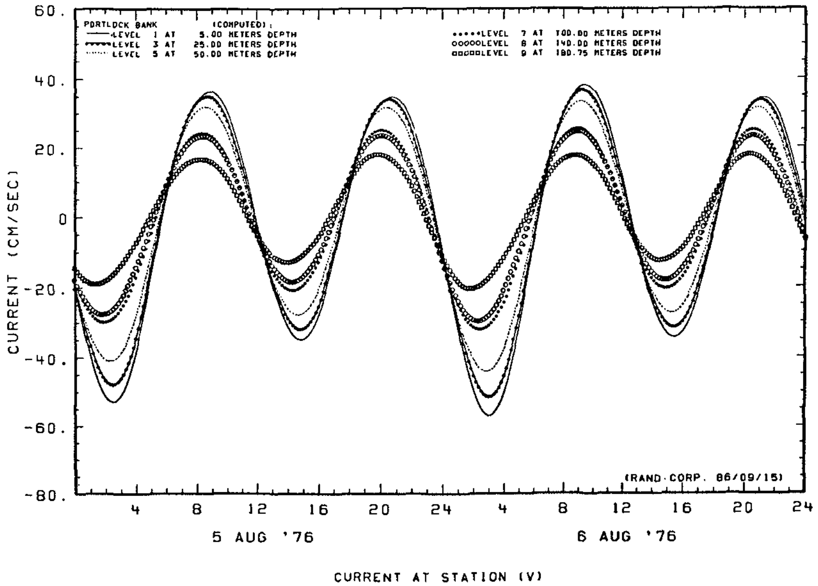

Fig. 6--The computed north-south velocity components at six representative layers near the mouth of Cook Inlet (Portlock Bank).

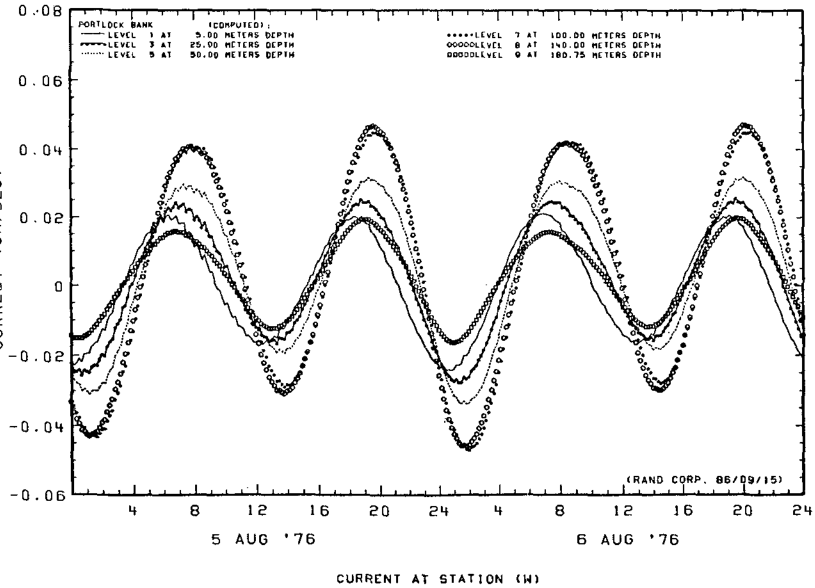

Fig. 7--The computed vertical velocity components at six representative layers near the mouth of Cook Inlet (Portlock Bank).

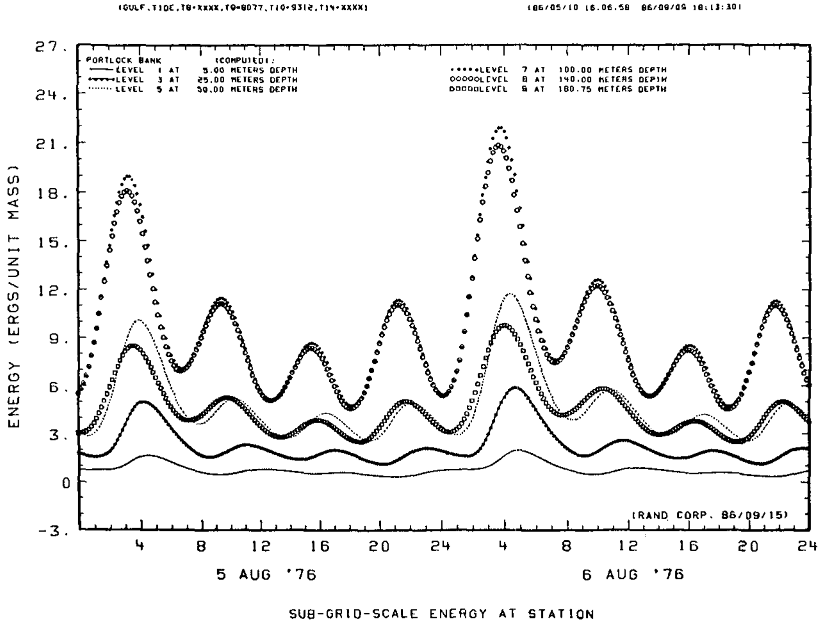

Fig. 8--The computed turbulent energy densities at six representative layers near the mouth of Cook Inlet (Portlock Bank).

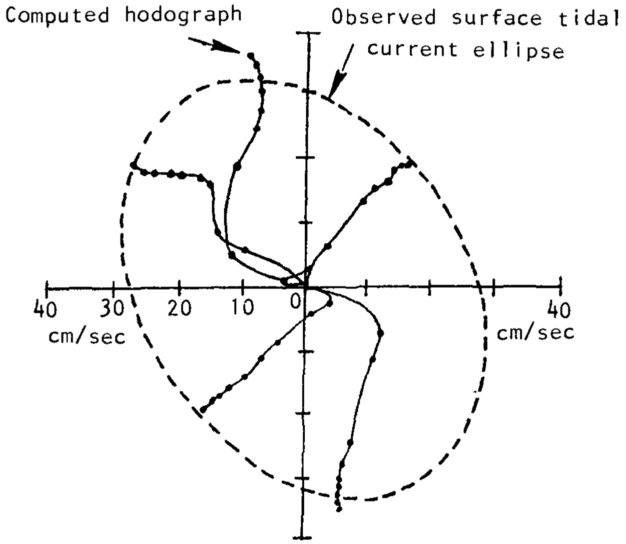

Comparison between the computed hodograph and the measured surface tidal current ellipse

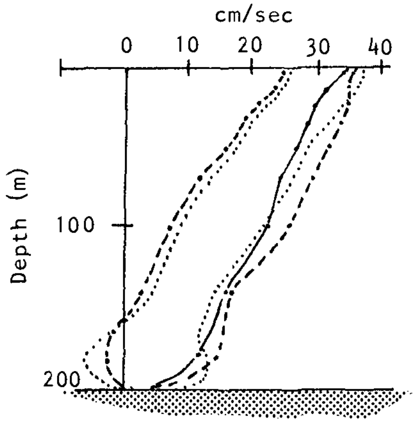

Vertical distribution of magnitude of the computed currents illustrated in the hodograph (near Cook Inlet)

Fig. 9

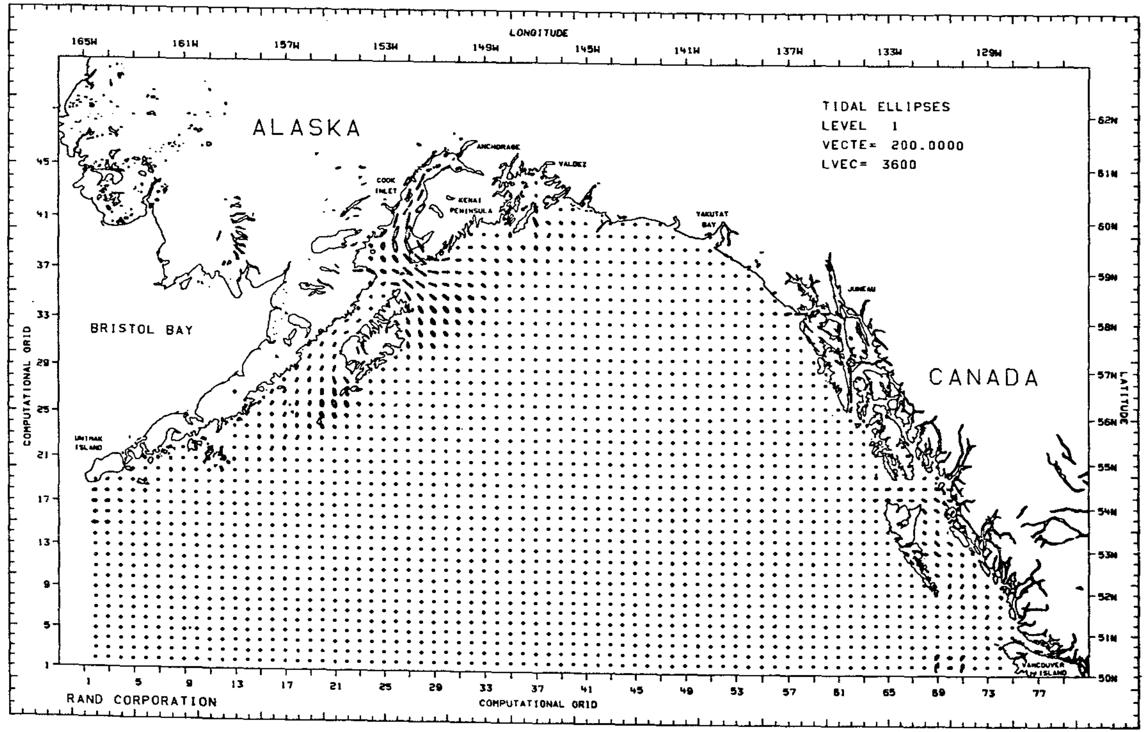

Fig. 10--Computed tidal ellipses in the Gulf of Alaska using a plotting scale of 200 cm/sec per grid spacing. Maximum tidal excursions are found in the middle Cook Inlet where the tidal currents can reach 140 cm/sec in either direction. Currents over the shelf-break near Kodiak are of elliptical rotary-type and can reach a maximum speed of 70 cm/sec.

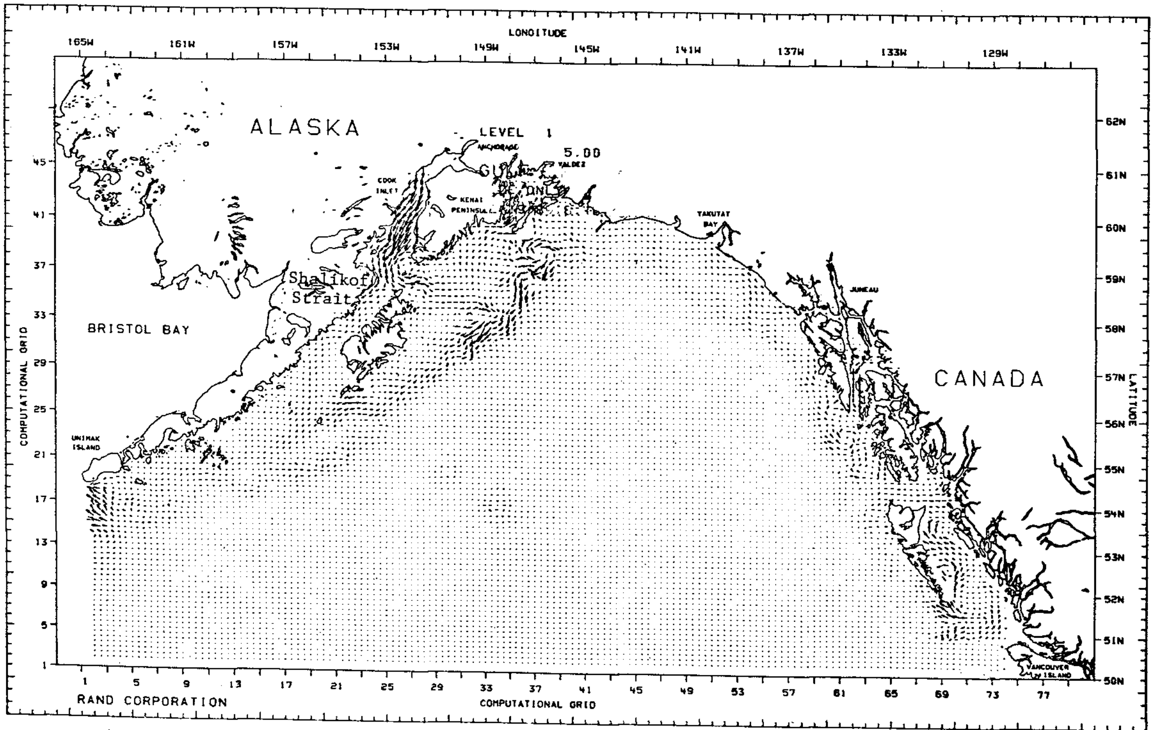

Fig. 11-- Computed tidal residual circulation in the Gulf of Alaska using a plotting scale of 5 cm/sec per computational grid. Maximum residual current in the middle Cook Inlet can reach a speed of 7.5 cm/sec which is approximately 5.5% of the local maximum tidal current. Over the shelf break and in the Shalikof Strait, residual currents flow primarily toward the southwest.

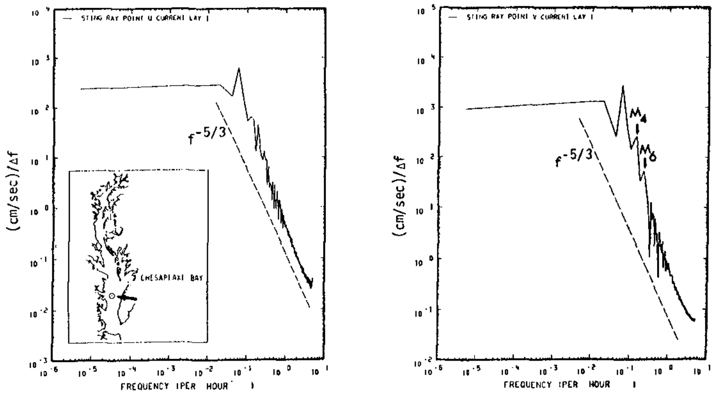

Driven only with M^2 tide (monochromatic wave) at the open boundary the proposed numerical scheme is capable of producing the cascade of energy distribution according to the universal "minus five-third" through the models nonlinear advective process (Hinze, 1959).

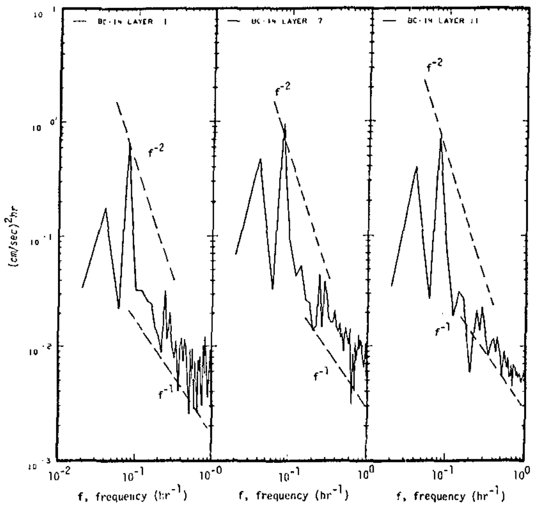

For the stratified fluid, the computed spectra of the vertical displacements (in the surface layer, within pycnocline and near bottom) and significant energy distribution agree with the observed spectra of the first mode of internal waves (Gordon, 1978).

Fig. 12

because coastal flows are primarily two-dimensional. Recent findings on the non-equilibrium statistical characteristics of turbulence have shown that even the universal Kolmogorof-constant of the tubulence spectrum has to be modified for two-dimensional turbulence. Models relying on the Richardson number-related parameters are specially susceptible to field measurement inaccuracies.

Consequently, over the past several years, we have modified our earlier models from requiring Richardson-number-related parameters to an energy balance approach. In the new method, the production and dissipation terms in the vertical energy turbulence-balance equation takes this form:

$$\bar{S}_e^z - D_e = \underbrace{a_3 \overline{L\sqrt{e}}^z \left[(\delta_z \overline{u}^x)^2 + (\delta_z \overline{V}^y)^2\right]}_{(1)} + \underbrace{a_3 \overline{L\sqrt{e}}^z \frac{g}{\overline{h}^z \rho} (\delta_z \overline{\rho}^z)}_{(2)} \underbrace{- a_2 e^{3/2}/L}_{(3)}$$

Where the first term denotes production, the second term represents the portion supplied that is used in potential energy increase, and the third term is dissipation. Some computational results are presented in Figs. 12 and 13. For example, when driven only with M2 tide (a monochromatic wave) at the open boundary, the numerical scheme is capable of producing the cascade of energy partition according to the universal "minus five-third" law through the model's non-linear advective process (top graphs of Fig. 12, also see the recent measurements by

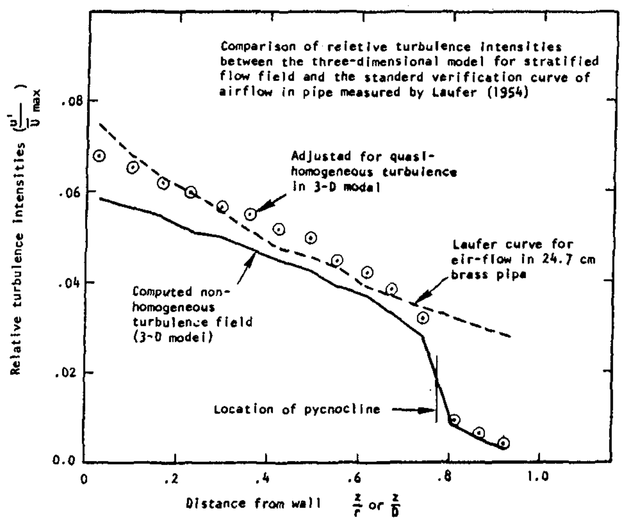

Fig. 13-- When the computed relative turbulence intensities at 15 layers are normalized with respect to the bottom distance, they are nearly the same when compared with the standard verification curve of airflow measured in brass pipe (made by Laufer for NACA, later NASA).

Heathershaw, 1979 and Elliott, 1984). Peaks of the spectra for two-dimensional turbulence are not uniquely located, however, it depends on the energy input and the relative location from the boundary (the so-called localization factor). The lower graphs of Fig 12 show the computed partitions of spectral energy of the vertical displacement near the pycnocline agree with the observed spectra of the first mode of internal waves (Gordon, 1978). When the computed relative turbulence intensities at various layers are normalized with respect to the bottom distance, they are nearly the same when compared with the NASA standard verification curve of airflow measured in brass pipe (made by Laufer). The insulation of momentum transfer across the pycnocline is evident . It is also clear that in stratified flows, more measurements and better model formulation are still needed.

Acknowledgments

This study was supported by the U. S. Bureau of Land Management through interagency agreement with the National Oceanic and Atmospheric Administration (NOAA), under which a multi-year program responding to needs of petroleum development of the Alaska Continental Shelf is managed by the Outer Continental Shelf Environmental Assessment Program Office.

Thanks go to our RAND colleagues Mr. A. B. Nelson and Mrs. G. Coughlan for their indispensable efforts in simulations and report preparation.

References

Elliott, A. J.,(1984): Measurements of the turbulence in an abyssal boundary layer, Jour. Physic. Oceano. Vol. 14, No.11, p 1779-1786.

Gordon, R. L.,(1978): Internal wave climate near the coast of Northwest Africa during JOINT-1, Deep Sea Res. Vol. 25, pp.625-643.

Hinze., J. O., (1959): Turbulence, McGraw-Hill, New York.

Heathershaw, A. D.,(1979): The turbulent structure of the bottom boundary layer in a tidal current. Geophys. J. Roy. Astron. Soc. Vol. 58, pp. 395-430.

Laufer, J.,(1954): The structure of turbulence in fully developed pipe flow, National Adv. Comm. on Aero., TR-1174.

Liu, S. K., and J. J. Leendertse, (1978): Multidimensional numerical modeling of estuaries and coastal seas, in Advances in Hydroscience. Vol 11, Academic Press. New York.

Schumacher, J. D., and R. D. Muench,(1980): Physical oceanography and meteorological conditions in the northwest Gulf of Alaska. NOAA TM-ERL-PMEL-22, Oct. 1980.